Two-dimensional active motion

Francisco J. Sevilla[1, *]

[1] *Instituto de Física, Universidad Nacional Autónoma de México,*
Apdo. Postal 20-364, 01000, Ciudad de México, México

(ΩDated: May 16, 2019)

The diffusion in two dimensions of non-interacting active particles that follow an arbitrary motility pattern is considered for analysis. Accordingly, the transport equation is generalized to take into account an arbitrary distribution of scattered angles of the swimming direction, which encompasses the pattern of motion of particles that move at constant speed. An exact analytical expression for the marginal probability density of finding a particle on a given position at a given instant, independently of its direction of motion, is provided; and a connection with a generalized diffusion equation is unveiled. Exact analytical expressions for the time dependence of the mean-square displacement and of the kurtosis of the distribution of the particle positions are presented. For this, it is shown that only the first trigonometric moments of the distribution of the scattered direction of motion are needed. The effects of persistence and of circular motion are discussed for different families of distributions of the scattered direction of motion.

I. INTRODUCTION

The intense study of the out-of-equilibrium systems called *active matter*, has allowed to set up a firm basis for the understanding of a variety of out-of-equilibrium phenomena. Even at the individual level of description, the intrinsic nonequilibrium nature of active motion leads to diverse phenomena not observed in particles that move passively. Furthermore, the great diversity of the patterns of self-propelled motion observed in biological organisms (see the introductory section in Refs. [1, 2]) or in artificially designed active particles [3], enriches the variety of effects exhibited by these systems .

A salient feature of active motion is that it is *persistent*, a characteristic that explicitly depends on the specific pattern of motion performed by the particle. The effects of persistence are well known, for instance, when active particles are confined to move under the effects of either an external potential or hard-walls, they lead to stationary distributions that differ from the expected ones. In the case of confined motion by trapping potentials, the effects of persistence lead to distributions that differ from the one given by Boltzmann and Gibbs [4–7]. Theoretical comparative studies that consider the two more studied patterns of motion –*active Brownian motion*, where the orientation of motion undergoes rotational diffusion, and *run-and-tumble motion*, which alternates running events with instantaneous, temporally uncorrelated tumbling events– reveal that, although there are important quantitative differences between them, they similarly behave in the long-time regime (normal diffusion) and have the same behavior in the short-time regime (ballistic motion). In the intermediate-time regime however, i.e., for times of the order of the *persistence time*, conspicuous differences are revealed between both patterns of motion [8].

Hence, to have at our disposal a theoretical framework that incorporates an arbitrary pattern of motion of active swimmers it is highly desirable. An important theoretical framework based on *continuous time random walks* has been known in the literature, and focuses on a family of patterns of motion characterized by the Poissonian or non-Poissonian statistics between turning events [1, 2, 9]. In this paper, I present a theoretical framework of two-dimensional motion of active swimmers, for a family of patterns of motion characterized by constant speed and an arbitrary probability distribution of the turning angle (scattered angle) of the swimming direction.

On the basis of the *transport equation* [10, 11], I introduce in section II such a framework, and present the corresponding Fokker-Planck equation for the probability density that at time t, a particle is located at $\boldsymbol{x}$ and moving along the direction $\hat{\boldsymbol{v}}$. Its general solution is presented in Sect. III. The marginal probability distribution of finding a swimmer at $\boldsymbol{x}$ at time t, independently of the direction of motion is of great interest, and in Sect. III I provide an exact solution, whose physical consequences are analyzed. A connection with a *generalized diffusion equation* is also unveiled. In section IV generalities, applications and predictions of the framework are presented for some general families of patterns of motion. Finally I give my concluding remarks in V.

II. THE TWO-DIMENSIONAL ACTIVE TRANSPORT EQUATION

The starting point is the two-dimensional equation for the probability density, $\mathcal{P}(\boldsymbol{x}, \varphi, t)$, of a single particle being at position $\boldsymbol{x}$, moving at constant speed v_0 along a direction given by the angle φ at time t, to say

$$\frac{\partial}{\partial t}\mathcal{P}(\boldsymbol{x}, \varphi, t) + v_0\hat{\boldsymbol{v}} \cdot \nabla\mathcal{P}(\boldsymbol{x}, \varphi, t) = D_T\nabla^2\mathcal{P}(\boldsymbol{x}, \varphi, t)$$

$$+ \int_{-\pi}^{\pi} d\varphi' K_A\left(\varphi|\varphi'\right)\mathcal{P}(\boldsymbol{x}, \varphi', t), \quad (1)$$

---

where the unit vector $\hat{\boldsymbol{v}}$ is defined by $(\cos\varphi, \sin\varphi)$, φ being the angle between the direction of motion and the horizontal axis of a given Cartesian reference frame. D_T is the translational diffusion coefficient that gives account of the thermal fluctuations exerted by the surrounding medium. The transition rate of the direction of motion, $K_A(\varphi|\varphi')$, gives the probability rate of the transition from the direction of motion φ' to φ, and encompasses the detailed information of a specific pattern of active motion considered. In this paper, I focus on the case in which $K_A(\varphi|\varphi')$ is independent of time, of the swimming speed and of the particle position. However, such dependences must be considered in the more general situations, as for instance in the case of the bacterium *Pseudomonas putida*, whose swimming speed depends, after a transition, on the selected direction of motion [12].

I refer to Equation (1) as the *active-transport equation*. The passive fluctuations exerted on the particle motion are separated from the active ones due to the time-scale disparity between them, which allows to write

$$\mathcal{P}(\boldsymbol{x}, \varphi, t) = \int d^2x' \, G_{D_T}(\boldsymbol{x} - \boldsymbol{x}', t) P(\boldsymbol{x}', \varphi, t), \quad (2)$$

where $G_D(\boldsymbol{x}, t)$ denotes the two-dimensional Gaussian propagator of the diffusion equation with diffusion coefficient D, given explicitly by $\exp\{-\boldsymbol{x}^2/4Dt\}/4\pi Dt$. The active part of motion is entailed by the probability density $P(\boldsymbol{x}', \varphi, t)$, which satisfy the gain-loss equation

$$\frac{\partial}{\partial t}P(\boldsymbol{x}, \varphi, t) + v_0\hat{\boldsymbol{v}}\cdot\nabla P(\boldsymbol{x}, \varphi, t) =$$
$$\int_{-\pi}^{\pi} d\varphi' Q(\varphi, \varphi') \, P(\boldsymbol{x}, \varphi', t)$$
$$-\left[\int_{-\pi}^{\pi} d\varphi' Q(\varphi', \varphi)\right] P(\boldsymbol{x}, \varphi, t), \quad (3)$$

when $K_A(\varphi|\varphi')$ is written in terms of the distribution of scattering-angle $Q(\varphi, \varphi')$ as

$$K_A(\varphi|\varphi') = Q(\varphi, \varphi') - \delta(\varphi - \varphi')\int_{-\pi}^{\pi} d\varphi'' Q(\varphi'', \varphi). \quad (4)$$

A further simplification can be realized by considering a rotationally invariant transition rate function, i.e., $Q(\varphi, \varphi') = Q(\varphi - \varphi')$. In such a case we can write [11]

$$\frac{\partial}{\partial t}P(\boldsymbol{x}, \varphi, t) + v_0\hat{\boldsymbol{v}}\cdot\nabla P(\boldsymbol{x}, \varphi, t) =$$
$$\Lambda\int_{-\pi}^{\pi} d\varphi' \widetilde{Q}(\varphi - \varphi') \, P(\boldsymbol{x}, \varphi', t)$$
$$-\Lambda P(\boldsymbol{x}, \varphi, t), \quad (5)$$

where $\Lambda \equiv \int_{-\pi}^{\pi} d\varphi' Q(\varphi')$ is the inverse of the time-scale that measures the average time between transitions, and $\widetilde{Q}(\varphi) = Q(\varphi)/\Lambda$.

III. THE GENERAL SOLUTION TO THE ACTIVE TRANSPORT EQUATION

We are interested in the analytical solutions, $P(\boldsymbol{x}, \varphi, t)$, if any, of Eq. (5), with the initial condition $P(\boldsymbol{x}, \varphi, 0) = \delta^{(2)}(\boldsymbol{x})/2\pi$, which corresponds to the case of an ensemble of independent active particles that depart from the origin in a Cartesian system of coordinates and propagates in a random direction of motion drawn from the uniform distribution in $[-\pi, \pi]$, $\delta^{(2)}(\boldsymbol{x})$ being the two dimensional Dirac's delta function.

Due to the assumed spatial isotropy of the system, I apply the Fourier transform to Eq. (5) and obtain

$$\frac{\partial}{\partial t}\widetilde{P}(\boldsymbol{k}, \varphi, t) + iv_0\hat{\boldsymbol{v}}\cdot\boldsymbol{k}\,\widetilde{P}(\boldsymbol{k}, \varphi, t) =$$
$$\Lambda\int_{-\pi}^{\pi} d\varphi' \widetilde{Q}(\varphi - \varphi')\,\widetilde{P}(\boldsymbol{k}, \varphi', t)$$
$$-\Lambda\widetilde{P}(\boldsymbol{k}, \varphi, t), \quad (6)$$

where

$$\widetilde{P}(\boldsymbol{k}, \varphi, t) = \int \frac{d^2x}{2\pi}\, e^{-i\boldsymbol{k}\cdot\boldsymbol{x}}\, P(\boldsymbol{x}, \varphi, t), \quad (7)$$

denotes the symmetric Fourier transform of $P(\boldsymbol{x}, \varphi, t)$ and $\boldsymbol{k} = (k_x, k_y)$, denotes the system's wave-vector. The following Fourier series expansion,

$$\widetilde{P}(\boldsymbol{k}, \varphi, t) = \frac{1}{2\pi}\sum_{n=-\infty}^{\infty} \widetilde{p}_n(\boldsymbol{k}, t)\, e^{-\lambda_n t}\, e^{in\varphi}, \quad (8)$$

is suitable since it fulfills the periodicity condition of the probability density, $\widetilde{P}(\boldsymbol{k}, \varphi, t) = \widetilde{P}(\boldsymbol{k}, \varphi + 2\pi, t)$.

The coefficients $\widetilde{p}_n(\boldsymbol{k}, t)$ in the expansion (8) are obtained by the use of the standard orthogonality relation among the Fourier basis functions $\{e^{in\varphi}\}$, explicitly

$$\widetilde{p}_n(\boldsymbol{k}, t) = \int \frac{d^2k}{2\pi}\, e^{-i\boldsymbol{k}\cdot\boldsymbol{x}}\, p_n(\boldsymbol{x}, t) \quad (9)$$

$$= e^{\lambda_n t}\int_{-\pi}^{\pi} d\varphi\, \widetilde{P}(\boldsymbol{k}, \varphi, t)e^{-in\varphi} \quad (10)$$

and satisfy the identity $\widetilde{p}^*_{-n}(\boldsymbol{k}, t) = \widetilde{p}_n(\boldsymbol{k}, t)$, since the probability density $P(\boldsymbol{x}, \varphi, t)$ is a real function.

The factors $e^{-\lambda_n t}$ in the expansion (8), correspond to the coefficients, $c_n(t)$, of the expansion in Fourier series of $f(\varphi, t)$ that solves the equation

$$\frac{\partial}{\partial t}f(\varphi, t) = \Lambda\int_{-\pi}^{\pi} d\varphi' \widetilde{Q}(\varphi - \varphi')\, f(\varphi', t) - \Lambda f(\varphi, t), \quad (11)$$

with λ_n a complex number given by

$$\lambda_n = \Lambda\left[1 - \langle e^{-in\varphi}\rangle_{\widetilde{Q}}\right], \quad (12)$$

where

$$\langle\Phi(\varphi)\rangle_{\widetilde{Q}} = \int_{-\pi}^{\pi} d\varphi\, \widetilde{Q}(\varphi)\Phi(\varphi) \qquad (13)$$

denotes the average of the φ-dependent quantity $\Phi(\varphi)$ computed by the use of the scattering-angle distribution $\widetilde{Q}(\varphi)$.

Accordingly, the main features of a particular pattern of active motion are encoded in the distribution of scattered angles $\widetilde{Q}(\varphi)$, which gives the particular orientation process of the swimming direction. Such features are equivalently inherited in the trigonometric moments:

$$\Gamma_n = \Lambda\left[1 - \langle\cos n\varphi\rangle_{\widetilde{Q}}\right], \qquad (14a)$$

$$\Omega_n = \Lambda\langle\sin n\varphi\rangle_{\widetilde{Q}}, \qquad (14b)$$

which correspond to the real and imaginary part of λ_n, respectively, thus $\lambda_n = \Gamma_n + i\,\Omega_n$. These quantities provide the relevant information about the diffusion process of active particles (see Refs. for the case of *correlated random walks* [13, 14]).

A series of properties for Γ_n and Ω_n can be deduced in a straightforward way. From the normalization of $\widetilde{Q}$ we have that $\Gamma_0 = \Omega_0 = 0$, and since $\widetilde{Q}(\varphi)$ is a real valued function, we have that the complex conjugate of λ_n is given by $\lambda_n^* = \lambda_{-n}$, which implies $\Gamma_n = \Gamma_{-n}$ and $\Omega_n = -\Omega_{-n}$. From this property one can show that the coefficients $\widetilde{p}_n(\boldsymbol{k}, t)$ of the expansion (15) satisfy $\widetilde{p}_{-n}(-\boldsymbol{k}, t) = \widetilde{p}_n^*(\boldsymbol{k}, t)$. Notice further that $0 \leq \Gamma_n \leq 2\Lambda$ and that $-\Lambda \leq \Omega_n \leq \Lambda$. With this observations, the expansion (8) can be explicitly split as

$$\widetilde{P}(\boldsymbol{k}, \varphi, t) = \frac{1}{2\pi}\widetilde{p}_0(\boldsymbol{k}, t) + \frac{1}{2\pi}\sum_{\substack{n=-\infty,\\ n\neq 0}}^{\infty} \widetilde{p}_n(\boldsymbol{k}, t)e^{-\Gamma_n t}e^{-i\Omega_n t}e^{in\varphi}. \quad (15)$$

Evidently, $P(\boldsymbol{x}, \varphi, t)$ tends asymptotically to $p_0(\boldsymbol{x}, t)/2\pi$ as time goes by.

A. The coefficients $p_n(\boldsymbol{x}, t)$

After substitution of Eq. (8) into Eq. (6), and use of the orthogonality of the Fourier basis functions, a set of coupled ordinary differential equations for the coefficients $\widetilde{p}_n(\boldsymbol{k}, t)$ is obtained, namely [15–17]

$$\frac{d}{dt}\widetilde{p}_n(\boldsymbol{k}, t) = -\frac{v_0}{2}ike^{\lambda_n t}\left[e^{-i\theta}\, e^{-\lambda_{n-1}t}\, \widetilde{p}_{n-1}(\boldsymbol{k}, t) + e^{i\theta}\, e^{-\lambda_{n+1}t}\, \widetilde{p}_{n+1}(\boldsymbol{k}, t)\right], \quad (16)$$

where θ and k correspond to the polar coordinates of the two-dimensional Fourier vector $\boldsymbol{k}$, i.e., $k_x \pm ik_y = ke^{\pm i\theta}$. Equations (16) are complemented by the initial conditions $\widetilde{p}_n^{(0)}(\boldsymbol{k}) = (2\pi)^{-1}\delta_{n,0}$, which are obtained straightforwardly from the initial distribution considered, i.e., $P(\boldsymbol{x}, \varphi, 0) = \delta^{(2)}(\boldsymbol{x})/2\pi$.

The first five coefficients, $p_0(\boldsymbol{x}, t)$, $p_{\pm 1}(\boldsymbol{x}, t)$ and $p_{\pm 2}(\boldsymbol{x}, t)$, in the position domain, can be related to: i) the probability density

$$\varrho(\boldsymbol{x}, t) = \frac{1}{2\pi}p_0(\boldsymbol{x}, t) = \frac{1}{2\pi}\int_{-\pi}^{\pi} d\varphi\, P(\boldsymbol{x}, \varphi, t); \qquad (17)$$

ii) the first-rank tensor $\boldsymbol{j}(\boldsymbol{x}, t)$ with components

$$j_x(\boldsymbol{x}, t) = \frac{1}{\pi}\mathrm{Re}[p_1(\boldsymbol{x}, t)e^{-\lambda_1 t}]$$
$$= \frac{1}{\pi}\int_{-\pi}^{\pi} d\varphi\, \cos\varphi\, P(\boldsymbol{x}, \varphi, t), \qquad (18a)$$
$$j_y(\boldsymbol{x}, t) = \frac{1}{\pi}\mathrm{Im}\left[p_{-1}(\boldsymbol{x}, t)e^{-\lambda_{-1}t}\right]$$
$$= \frac{1}{\pi}\int_{-\pi}^{\pi} d\varphi\, \sin\varphi\, P(\boldsymbol{x}, \varphi, t), \qquad (18b)$$

from which the probability density current $\boldsymbol{J}(\boldsymbol{x}, t) = \frac{v_0}{2}\boldsymbol{j}(\boldsymbol{x}, t)$ is introduced; and iii) the traceless, symmetric, 2×2 second-rank tensor $\mathbb{W}(\boldsymbol{x}, t)$, whose entries are given by

$$\mathbb{W}_{xx}(\boldsymbol{x}, t) = -\mathbb{W}_{yy}(\boldsymbol{x}, t)$$
$$= \frac{1}{\pi}\mathrm{Re}\left[p_2(\boldsymbol{x}, t)e^{-\lambda_2 t}\right]$$
$$= \frac{1}{\pi}\int_{-\pi}^{\pi} d\varphi\, \cos 2\varphi\, P(\boldsymbol{x}, \varphi, t), \qquad (19a)$$
$$\mathbb{W}_{xy}(\boldsymbol{x}, t) = \mathbb{W}_{yx}(\boldsymbol{x}, t)$$
$$= \frac{1}{\pi}\mathrm{Im}\left[p_{-2}(\boldsymbol{x}, t)e^{-\lambda_{-2}t}\right]$$
$$= \frac{1}{\pi}\int_{-\pi}^{\pi} d\varphi\, \sin 2\varphi\, P(\boldsymbol{x}, \varphi, t). \qquad (19b)$$

B. The probability density $p_0(\boldsymbol{x}, t)$

As in previous studies, the probability density of finding a particle at position $\boldsymbol{x}$, independently of its direction of motion, $p_0(\boldsymbol{x}, t)$, is of interest. After transforming the time domain to the Laplace domain, an exact solution for $\widetilde{p}_0(\boldsymbol{k}, \epsilon)$ can be obtained from Eq. (16) in the form of continuous fractions, namely

$$\widetilde{p}_0(\boldsymbol{k}, \epsilon) = \widetilde{p}_0^{(0)}(\boldsymbol{k}) \cfrac{1}{\epsilon + \cfrac{(v_0/2)^2 \boldsymbol{k}^2}{\epsilon + \lambda_1 + \cfrac{(v_0/2)^2 \boldsymbol{k}^2}{\epsilon + \lambda_2 + \cfrac{(v_0/2)^2 \boldsymbol{k}^2}{\epsilon + \lambda_3 + \ddots}}} + \cfrac{(v_0/2)^2 \boldsymbol{k}^2}{\epsilon + \lambda_1^* + \cfrac{(v_0/2)^2 \boldsymbol{k}^2}{\epsilon + \lambda_2^* + \cfrac{(v_0/2)^2 \boldsymbol{k}^2}{\epsilon + \lambda_3^* + \ddots}}}}, \tag{20}$$

where the explicit dependence on the variable ϵ conveys that the Laplace transform $\left[f(\epsilon) = \int_0^\infty dt\, e^{-\epsilon t} f(t)\right]$ has been carried out, and $\widetilde{p}_0^{(0)}(\boldsymbol{k})$ denotes the initial distribution $\widetilde{p}_0(\boldsymbol{k}, t = 0)$. The solution (20) is akin to the solution found in Ref. [18] for end-to-end distribution of a wormlike chain as has been pointed in Ref. [19]. In the present paper the meaning of the solution (20) can be elucidated after rewritten it as

$$\widetilde{p}_0(\boldsymbol{k}, \epsilon) = \frac{\widetilde{p}_0^{(0)}(\boldsymbol{k})}{\epsilon + (v_0/2)^2 \, \boldsymbol{k}^2 \, \widetilde{\mathfrak{D}}(\boldsymbol{k}, \epsilon)}, \tag{21}$$

or equivalently as

$$\epsilon \widetilde{p}_0(\boldsymbol{k}, \epsilon) - \widetilde{p}_0^{(0)}(\boldsymbol{k}) = -\left(\frac{v_0}{2}\right)^2 \, \boldsymbol{k}^2 \, \widetilde{\mathfrak{D}}(\boldsymbol{k}, \epsilon) \widetilde{p}_0(\boldsymbol{k}, \epsilon), \tag{22}$$

which can be recognized as the Fourier-Laplace transform of the spatially-non-local *generalized diffusion equation*,

$$\frac{\partial}{\partial t} p_0(\boldsymbol{x}, t) = \left(\frac{v_0}{2}\right)^2 \int d^2 x' \int_0^t ds\, \mathfrak{D}(\boldsymbol{x} - \boldsymbol{x}', t - s) \nabla'^2 p_0(\boldsymbol{x}', s), \tag{23}$$

introduced in Ref. [20] and used in the context of animal motion with internal states in [21]. The *connecting function* $\mathfrak{D}(\boldsymbol{x}, t)$ is given explicitly in the Fourier-Laplace domain by

$$\widetilde{\mathfrak{D}}(\boldsymbol{k}, \epsilon) = \cfrac{1}{\epsilon + \lambda_1 + \cfrac{(v_0/2)^2 \boldsymbol{k}^2}{\epsilon + \lambda_2 + \cfrac{(v_0/2)^2 \boldsymbol{k}^2}{\epsilon + \lambda_3 + \ddots}}} + \cfrac{1}{\epsilon + \lambda_1^* + \cfrac{(v_0/2)^2 \boldsymbol{k}^2}{\epsilon + \lambda_2^* + \cfrac{(v_0/2)^2 \boldsymbol{k}^2}{\epsilon + \lambda_3^* + \ddots}}}. \tag{24}$$

We introduce the recursive relations

$$\Delta_n(\boldsymbol{k}, \epsilon) = \frac{1}{\epsilon + \lambda_{n+1} + (v_0/2)^2 \boldsymbol{k}^2 \Delta_{n+1}(\boldsymbol{k}, \epsilon)}, \tag{25a}$$

$$\overline{\Delta}_n(\boldsymbol{k}, \epsilon) = \frac{1}{\epsilon + \lambda_{-(n+1)} + (v_0/2)^2 \boldsymbol{k}^2 \overline{\Delta}_{n+1}(\boldsymbol{k}, \epsilon)}, \tag{25b}$$

for $n \geq 0$, to write Eq. (24) in a simplified form as

$$\widetilde{\mathfrak{D}}(\boldsymbol{k}, \epsilon) = \Delta_0(\boldsymbol{k}, \epsilon) + \overline{\Delta}_0(\boldsymbol{k}, \epsilon). \tag{26}$$

In the asymptotic limit, i.e., in the long-time regime, $\epsilon \to 0$, and in the short-wave-vector limit, $k = |\boldsymbol{k}| \to 0$, the connecting function is given by the zeroth order *approximant*, $\widetilde{\mathfrak{D}}^{(0)}(\epsilon)$, obtained after evaluating $\widetilde{\mathfrak{D}}(\boldsymbol{k}, \epsilon)$ at $\boldsymbol{k} = \boldsymbol{0}$, i.e.,

$$\widetilde{\mathfrak{D}}^{(0)}(\epsilon) \equiv \widetilde{\mathfrak{D}}(\boldsymbol{0}, \epsilon) = \frac{1}{\epsilon + \lambda_1} + \frac{1}{\epsilon + \lambda_1^*}. \tag{27}$$

This implies a spatially-local connecting function, that exhibits oscillations of frequency Ω_1, exponentially damped with relaxation time Γ_1^{-1}, namely

$$\mathfrak{D}^{(0)}(\boldsymbol{x}, t) = 2\delta^2(\boldsymbol{x}) e^{-\Gamma_1 t} \cos \Omega_1 t. \tag{28}$$

With this approximation of the connecting function, we have that Eq. (23) can be rewritten in the form

$$\frac{\partial}{\partial t} p_0(\boldsymbol{x}, t) = \frac{v_0^2}{2} \int_0^t ds\, e^{-\Gamma_1(t-s)} \cos[\Omega_1(t-s)] \, \nabla^2 p_0(\boldsymbol{x}, s), \tag{29}$$

which corresponds to a generalization of the telegrapher equation in that it incorporates the effects of an effective torque that gives rise to circular motion of *angular speed* Ω_1. If $\Omega_1 = 0$, Eq. (29) reduces to the standard telegrapher's equation [22]

$$\frac{\partial^2}{\partial t^2} p_0(\boldsymbol{x}, t) + \Gamma_1 \frac{\partial}{\partial t} p_0(\boldsymbol{x}, t) = \frac{v_0^2}{2} \nabla^2 p_0(\boldsymbol{x}, s), \tag{30}$$

where the diffusion coefficient due to the persistence of the swimming direction, $D_{\text{pers}} = v_0^2/2\Gamma_1$, is apparent.

In advance, I identify Γ_1^{-1} with the *persistence time*. In the temporal asymptotic limit we have, from (20), that $\widetilde{p}_0(\boldsymbol{k},\epsilon) \sim \left[\epsilon + (v_0/2)^2\boldsymbol{k}^2\left(\lambda_1^{-1} + \lambda_1^{*-1}\right)\right]^{-1}$, which can be inverted straightforwardly to the spatial and temporal variables to give the Gaussian $G_{D_{\text{eff}}}(\boldsymbol{x},t)$, i.e.,

$$p_0(\boldsymbol{x},t) \sim \frac{1}{4\pi D_{\text{eff}}t}\exp\left\{-\frac{\boldsymbol{x}^2}{4D_{\text{eff}}t}\right\}. \qquad (31)$$

where the effective diffusion coefficient, D_{eff}, due to active motion is defined by $D_{\text{eff}} = D_{\text{pers}}/(1 + \Omega_1^2/\Gamma_1^2)$, which reduces to D_{pers} when Ω_1 vanishes.

On the other hand, in the short time regime ($|\epsilon| \gg |\lambda_n|$ for all n), we have that $\widetilde{p}_0(\boldsymbol{k},\epsilon)$ can be approximated by $\widetilde{p}_0^{(0)}(\boldsymbol{k})\left[1/\epsilon - 2(v_0/2)^2\boldsymbol{k}^2/\epsilon^3 + \ldots\right]$. After taking the inverse Laplace transformation we obtain

$$\widetilde{p}_0(\boldsymbol{k},t) \simeq \widetilde{p}_0^{(0)}(\boldsymbol{k})J_0(kv_0t), \qquad (32)$$

that results from identifying the first two terms of the power series of the zeroth-order Bessel function of the first kind $J_0(x) = 1 - (x/2)^2 + \ldots$. For the initial distribution considered, we obtain the radial pulse:

$$p_0(\boldsymbol{x},t) \simeq \frac{\delta(x - v_0t)}{2\pi x} \qquad (33)$$

that propagates at speed v_0 free of the wakes exhibited by the solution of the approximated description given by the telegrapher's equation in the short time regime [15], where $x = \|\boldsymbol{x}\|$.

The next order approximant of $\widetilde{\mathfrak{D}}(\boldsymbol{k},\epsilon)$ is of particular interest since it leads to a connecting function coupled in the spactail and temporal variables. Some models of stochastic motion consider memory functions that couple space and time, as is the case for the family of stochastic motion known as *Lévy walks* –described within the formalism of *continuous time random walks*– where the transition probability density that connects two distinct points in space at different times is constrained by the condition that the walker moves at constant speed [23]. In our case the first order approximant, $\widetilde{\mathfrak{D}}^{(1)}(\boldsymbol{k},\epsilon)$, is obtained from $\widetilde{\mathfrak{D}}(\boldsymbol{k},\epsilon)$ after evaluating $\Delta_1(\boldsymbol{k},t)$ and $\overline{\Delta}_1(\boldsymbol{k},\epsilon)$ at $\boldsymbol{k} = \boldsymbol{0}$, which leads to

$$\widetilde{\mathfrak{D}}^{(1)}(\boldsymbol{k},\epsilon) = \frac{1}{\epsilon + \lambda_1 + \dfrac{(v_0/2)^2\boldsymbol{k}^2}{\epsilon + \lambda_2}} + \frac{1}{\epsilon + \lambda_1^* + \dfrac{(v_0/2)^2\boldsymbol{k}^2}{\epsilon + \lambda_2^*}}. \tag{34}$$

In the time regime for which $|\epsilon| \ll |\lambda_2|$, an explicit simple expression for $\mathfrak{D}^{(1)}(\boldsymbol{x},t)$ in spatial and temporal coordinates is obtained, namely

$$\mathfrak{D}^{(1)}(\boldsymbol{x},t) = 2e^{-\Gamma_1 t}G_{v_0^2/4\Gamma_2}(\boldsymbol{x},t)\times$$
$$\left\{\cos\left[\Omega_1 t\left(1 + \frac{\Omega_2}{\Omega_1}\frac{\boldsymbol{x}^2}{v_0^2t^2}\right)\right] + \right.$$
$$\left. \frac{\Omega_2}{\Gamma_2}\sin\left[\Omega_1 t\left(1 + \frac{\Omega_2}{\Omega_1}\frac{\boldsymbol{x}^2}{v_0^2t^2}\right)\right]\right\}. \tag{35}$$

Due to the explicit appearance of the Gaussian $G_{v_0^2/4\Gamma_2}(\boldsymbol{x},t)$, the connecting function (35) gives a major contribution to those spatial positions $\boldsymbol{x}$, $\boldsymbol{x}'$, whose separation is less or of the order of the distance $\sqrt{v_0^2t/\Gamma_2}$, and decays quickly to zero for pairs of points whose distance is larger than this. It is expected, that the Gaussian nonlocality of (35) is a consequence of the approximation made, and that a connecting function that vanishes for pair of points whose distance is larger than v_0t is more appropriate. Note that (35) reduces to the long-time approximation given by (28), by taking the limit $\Omega_2, \Gamma_2 \to 0$.

C. The connecting function $\widetilde{\mathfrak{D}}(\boldsymbol{k},\epsilon)$ and the moments of $p_0(\boldsymbol{x},t)$

For the initial condition considered, we have that the solution given in Eq. (21) is a rotationally symmetric function that depends solely on $\boldsymbol{k}^2$, and we simply write $\widetilde{p}_0(k,\epsilon)$. Likewise, we can write $p_0(\boldsymbol{x},\epsilon) = (2\pi)^{-1}p_0(x,\epsilon)$, where x denotes the magnitude of $\boldsymbol{x}$, and the explicit appearance of the Laplace variable ϵ indicates that the Laplace transform is considered. The mentioned rotational symmetry allows to write

$$\widetilde{p}_0(k,\epsilon) = \frac{1}{2\pi}\sum_{n=0}^{\infty}\frac{(-1)^n}{(n!)^2}\frac{k^{2n}}{2^{2n}}\langle x^{2n}(\epsilon)\rangle_{\text{rad}}, \qquad (36)$$

where $\langle z[x(\epsilon)]\rangle_{\text{rad}}$ denotes the average of $z(x)$ over the radial distribution $x\,p_0(x,\epsilon)$, i.e., the rotationally symmetric moments are given by

$$\langle x^{2n}(\epsilon)\rangle_{\text{rad}} = \int_0^{\infty}dx\,x^{2n}\,x\,p_0(x,\epsilon), \qquad (37)$$

and obtained directly from $\widetilde{p}_0(k,\epsilon)$ from the formula

$$\langle x^{2n}(\epsilon)\rangle_{\text{rad}} = 2\pi\frac{(-1)^n n!\,2^n}{(2n-1)!!}\left.\frac{d^{2n}}{dk^{2n}}\widetilde{p}_0(k,\epsilon)\right|_{k=0}. \qquad (38)$$

1. The mean-square displacement

The mean-square displacement is defined by $\langle \boldsymbol{x}^2(t)\rangle$, which coincides with $\langle x^2(t)\rangle_{\text{rad}}$. It follows straightforwardly from (38), that the Laplace transform of the mean-square displacement is given by

$$\langle \boldsymbol{x}^2(\epsilon)\rangle = \frac{v_0^2}{\epsilon^2}\left.\widetilde{\mathfrak{D}}(\boldsymbol{k},\epsilon)\right|_{k=0} = \frac{v_0^2}{\epsilon^2}\widetilde{\mathfrak{D}}^{(0)}(\epsilon), \qquad (39)$$

since $\left.\widetilde{\mathfrak{D}}(\boldsymbol{k},\epsilon)\right|_{k=0}$ corresponds to the zeroth-order approximant $\widetilde{\mathfrak{D}}^{(0)}(\epsilon)$ of $\widetilde{\mathfrak{D}}(\boldsymbol{k},\epsilon)$, given in (27). After inverting the Laplace transform, the exact time dependence of
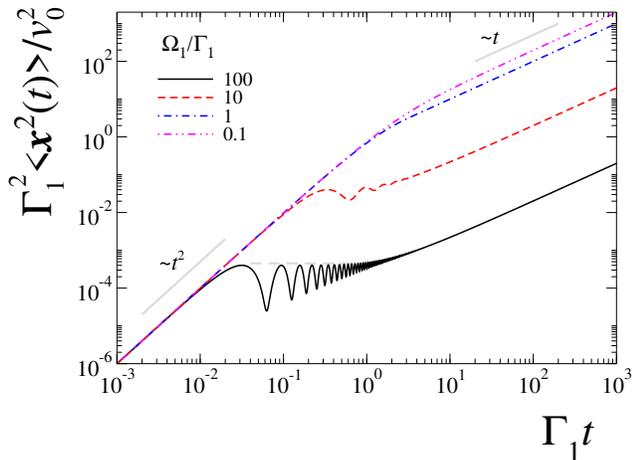
FIG. 1. (Color online) Dimensionless mean-square displacement $\Gamma_1^2\langle\boldsymbol{x}^2(t)\rangle/v_0^2$ as function of the dimensionless time $\Gamma_1 t$ for different values of the ratio Ω_1/Γ_1, namely, 0.1, 1, 10, 100.

the mean-square displacement is given by

$$\langle\boldsymbol{x}^2(t)\rangle = 4\frac{D_{\text{eff}}}{\Gamma_1}\left[\Gamma_1 t - \frac{1-\frac{\Omega_1^2}{\Gamma_1^2}}{1+\frac{\Omega_1^2}{\Gamma_1^2}}\left(1 - e^{-\Gamma_1 t}\cos\Omega_1 t\right)\right.$$
$$\left. - \frac{2\frac{\Omega_1}{\Gamma_1}}{1+\frac{\Omega_1^2}{\Gamma_1^2}}e^{-\Gamma_1 t}\sin\Omega_1 t\right], \quad (40)$$

which reduces to the well-known expression

$$\langle\boldsymbol{x}^2(t)\rangle = \frac{2v_0^2}{\Gamma_1^2}\left[\Gamma_1 t - \left(1 - e^{-\Gamma_1 t}\right)\right], \quad (41)$$

when Ω_1 vanishes.

From expression (40), the regime for which the particle motion is dominantly ballistic, $\langle\boldsymbol{x}^2(t)\rangle \to v_0^2 t^2$, is clearly obtained in the short-time regime, $\Gamma_1 t \ll 1$, for arbitrary Ω_1 (see Fig. 1). In contrast, in the long-time regime, $\Gamma_1 t \gg 1$, we get the standard linear dependence in time of the mean-square displacement

$$\langle\boldsymbol{x}^2(t)\rangle \sim 4D_{\text{eff}}\,t, \quad (42)$$

with D_{eff}, given as before, as $D_{\text{pers}}/(1 + \Omega_1^2/\Gamma_1^2)$. As is well-known [24, 25], the effective diffusion coefficient reaches its maximum value

$$D_{\text{eff}}^* = v_0^2/4\Omega_1 \quad (43)$$

at the ratio $\Omega_1/\Gamma_1 = 1$. It can be clearly noticed from Eq. (40), that the time dependence of the mean-square displacement depends only on the ratio Ω_1^2/Γ_1^2, whose explicit value depends on the particular transition probability density $\widetilde{Q}(\varphi)$. Thus, the crossover from the ballistic regime to the normal diffusion one, is sensitive to the particular details of the pattern of active motion,

entailed in Ω_1/Γ_1 through $\widetilde{Q}(\varphi)$ as is shown in Fig. 1. For large values of the ratio Ω_1/Γ_1, the particle get self-trapped in the intermediate-time regime due to the circular motion induced by the particular choice of $\widetilde{Q}(\varphi)$, and revealed by the corresponding oscillations of the mean-square displacement (see the solid-black line in Fig. 1 for $\Omega_1/\Gamma_1 = 100$).

2. The kurtosis

The non-Gaussian feature of the probability density $p_0(\boldsymbol{x}, t)$ can be characterized by its kurtosis κ, which as a matter of convenience, the definition given by Mardia [26] is used, namely

$$\kappa(t) = \left\langle\left[\left(\boldsymbol{x}(t)-\langle\boldsymbol{x}(t)\rangle\right)\Sigma^{-1}\left(\boldsymbol{x}(t)-\langle\boldsymbol{x}(t)\rangle\right)^{\text{T}}\right]^2\right\rangle, \quad (44)$$

where $\boldsymbol{x}^{\text{T}}$ denotes the transpose of the vector $\boldsymbol{x}$ and Σ is the 2×2 matrix defined by the average of the dyadic product $\left(\boldsymbol{x}(t)-\langle\boldsymbol{x}(t)\rangle\right)^{\text{T}}\cdot\left(\boldsymbol{x}(t)-\langle\boldsymbol{x}(t)\rangle\right)$. For the circularly symmetric case, the one considered in this paper, Eq. (44) reduces to

$$\kappa(t) = 4\frac{\langle x^4(t)\rangle_{\text{rad}}}{\langle x^2(t)\rangle_{\text{rad}}^2}. \quad (45)$$

From Eq. (38) we have that the Laplace transform of the time dependence of the fourth-moment is given by

$$\langle x^4(\epsilon)\rangle_{\text{rad}} = \frac{4v_0^4}{\epsilon^3}\left[\widetilde{\mathfrak{D}}(\boldsymbol{k},\epsilon)\right]_{k=0}^2 - \frac{8v_0^2}{\epsilon^2}\left[\frac{\partial^2}{\partial k^2}\widetilde{\mathfrak{D}}(\boldsymbol{k},\epsilon)\right]_{k=0}. \quad (46)$$

Note that from Eq. (27), the first term in the last equation depends solely on λ_1, λ_1^*, while the second term carries information about λ_2, λ_2^* since, as can be shown straightforwardly from (24) and (25),

$$\frac{\partial^2}{\partial k^2}\widetilde{\mathfrak{D}}(\boldsymbol{k},t)\bigg|_{k=0} = -\frac{v_0^2}{2}\left[\frac{1}{(\epsilon+\lambda_1)^2(\epsilon+\lambda_2)} + \frac{1}{(\epsilon+\lambda_1^*)^2(\epsilon+\lambda_2^*)}\right]. \quad (47)$$

Thus the fourth moment in Laplace domain is explicitly given by

$$\langle x^4(\epsilon)\rangle = \frac{4v_0^4}{\epsilon^2}\left[\frac{1}{\epsilon}\left(\frac{1}{\epsilon+\lambda_1}+\frac{1}{\epsilon+\lambda_1^*}\right)^2 + \frac{1}{(\epsilon+\lambda_1)^2(\epsilon+\lambda_2)} + \frac{1}{(\epsilon+\lambda_1^*)^2(\epsilon+\lambda_2^*)}\right]. \quad (48)$$

The general explicit time dependence of the fourth moment is too involved to be discussed at this point. Besides, the values of Γ_1, Ω_1, Γ_2 and Ω_2 are not independent among them, but they are related through the transition probability density $\widetilde{Q}(\varphi)$. Thus, an analysis of the

time dependence of the kurtosis is presented in the next section for particular cases of $\widetilde{Q}(\varphi)$. Notwithstanding this, the short- and long-time regimes can be discussed straightforwardly.

In the long-time regime ($|\epsilon| \ll |\lambda_1|, |\lambda_2|$), the second and third terms in the squared brackets of Eq. (48) can be neglected, and thus, it is the first term the one that mainly contributes in the long-time regime. In such regime the fourth moment is independent of λ_2 and λ_2^*, and the inversion of the Laplace transform can be done straightforwardly, which gives

$$\langle x^4(t) \rangle \sim 8 \frac{v_0^4 \Gamma_1^2}{\left(\Gamma_1^2 + \Omega_1^2\right)^2} t^2, \tag{49}$$

and from this, we can observe that $\kappa \sim 8$, which uniquely characterizes the two-dimensional Gaussian distribution. Unlike this case, in the short-time regime ($|\epsilon| \gg |\lambda_1|, |\lambda_2|$), we have that all the terms in Eq. (48) contribute, and such expression reduces to $4! v_0^4/\epsilon^5$, which can be inverted straight away to give $v_0^4 t^4$ (independent of λ_1, λ_2 and their complex conjugates), and thus $\kappa \simeq 4$ which characterizes the propagating pulse $\delta(x - v_0 t)/(2\pi x)$ [15, 16].

The effects of λ_2, λ_2^* can be observed only in the intermediate-time regime, where the particle positions distribution suffers of the important effects of persistence, as discussed in the following sections.

IV. PERSISTENCE TIME, NATURAL PERIOD OF ROTATION AND OTHER TIME-SCALES

As has been already introduced in Sect. III, the *persistence time* of the swimming direction, Γ_1^{-1}, and the *natural period* of the circular motion, Ω_1^{-1}, correspond to the relevant time-scales that define the diffusive regime of the active motion [see Eq. (42)]. Γ_1^{-1} is closely related to the persistence time introduced by Wu *et al.* in Ref. [27], and by Bartumeus *et al.* in Ref. [14] in the modeling and analysis of animal motion in two dimensions as correlated random walks. All the other time-scales that appear in the present analysis [see, for instance, the expansion Eq. (15)], namely, Γ_n^{-1}, Ω_n^{-1}, with $n > 1$, determine the precise statistical properties of active motion. These depend on the particular choice of the scattering-angle distribution $\widetilde{Q}(\varphi)$.

The simplest scattering-angle distribution may correspond to the case when $\widetilde{Q}(\varphi)$ is uniform in $[-\pi, \pi]$, i.e., $\widetilde{Q}(\varphi) = (2\pi)^{-1}$. This has been used to model the paradigmatic two-dimensional *run-and-tumble* pattern of active motion [6, 11, 28, 29], for which $\Gamma_n = \Lambda$ for all n, i.e., Λ is the unique time-scale that defines the dynamics of the swimming direction, meaning that all Fourier modes in the series (8) decay at the same pace Λ.

Moreover, many scattering-angle distributions can be built on by *wrapping* out a standard single-variate distribution, $\rho(\eta)$, with support on the interval $(-\infty, \infty)$, to the unitary circle, namely

$$\widetilde{Q}_{\mathrm{wr}}(\varphi) = \int_{-\infty}^{\infty} d\eta\, \rho(\eta) \sum_{m=-\infty}^{\infty} \delta(\eta - \varphi + 2\pi m). \tag{50}$$

One important set of scattering-angle distributions obtained in this manner, is got from the well-known Lévy alpha-stable distributions with index α, $\rho_{\alpha;\sigma,\phi,\beta}(\eta)$, whose characteristic function is given by

$$\hat{\rho}_{\alpha;\sigma,\phi,\beta}(\kappa) = \exp\left\{ i\kappa\phi - |\sigma\kappa|^\alpha \left(1 - i\beta \mathrm{sign}(\kappa)\right)\Phi \right\}, \tag{51}$$

being $\sigma > 0$ the width, ϕ the mode, and β the skewness, Φ equals $\tan(\pi\alpha/2)$ if $\alpha \neq 1$ and $-2\ln|\kappa|/\pi$ if $\alpha = 1$. The cases $\alpha = 2$; $\alpha = 1$, $\beta = 0$, and $\alpha = 1/2$, $\beta = 1$, are of interest, since these cases correspond to the wrapped Gaussian distribution, the wrapped Lorentz (Cauchy) distribution and the wrapped Lévy distribution, respectively. For this latter case, it is possible to obtain explicit expressions for Γ_n and Ω_n, we have for $n > 1$ that

$$\Gamma_n = \Lambda\left[1 - e^{-(\sigma n)^\alpha} \cos\left(n\phi + (\sigma n)^\alpha \beta\Phi\right)\right], \tag{52a}$$

$$\Omega_n = \Lambda e^{-(\sigma n)^\alpha} \sin\left(n\phi + (\sigma n)^\alpha \beta\Phi\right). \tag{52b}$$

Another important family of scattering-angle distributions is the one given by the angle distribution of Jones and Pewsey, $\widetilde{Q}_{\mathrm{JP},\sigma,\phi,\psi}(\varphi)$ [30], with parameters: $\sigma > 0$, ϕ, and $\psi \in (-\infty, \infty)$, which correspond respectively to the distribution width, the location of the unique mode, and the shape parameter. It has the explicit representation

$$\widetilde{Q}_{\mathrm{JP},\sigma,\phi,\psi}(\varphi) = \frac{\left[\cosh(\sigma\psi) + \sinh(\sigma\psi)\cos(\varphi - \phi)\right]^{1/\psi}}{2\pi P_{1/\psi}\left[\cosh(\sigma\psi)\right]}, \tag{53}$$

where $P_\gamma(z)$ is the associated Legendre function of the first kind of degree γ. The distribution (53) contains as particular cases [30]: the angle distribution of von Misses ($\psi = 0$)

$$\widetilde{Q}_{\mathrm{vM}}(\varphi) = \frac{e^{\kappa\cos\varphi}}{2\pi I_0(\kappa)}, \tag{54}$$

the cardioid distribution ($\psi = -1$)

$$\widetilde{Q}_{\mathrm{CD}}(\varphi) = \frac{1}{2\pi}\left(1 + \tanh(\kappa)\cos\varphi\right), \tag{55}$$

and the wrapped Cauchy distribution ($\psi = 1$)

$$\widetilde{Q}_{\mathrm{C}}(\varphi) = \frac{1}{2\pi} \frac{1 - \tanh^2(\frac{\kappa}{2})}{1 + \tanh^2(\frac{\kappa}{2}) - 2\tanh(\frac{\kappa}{2})\cos\varphi}. \tag{56}$$

The distribution (53) has also been used in the analysis of correlated random walks [14].

Though the number of possibilities to make the choice of the turning-angle distribution is huge, we focus our analysis on two wide-enough classes of the scattering functions: a class of unimodal distributions and one of bimodal distributions. Subclasses will be defined by features such as the symmetry with respect the turning angle zero, and will dress with specific properties to the quantities Γ_n and Ω_n.

A. Unimodal angular distributions

Lets first consider the case of unimodal distributions, which splits into two wide categories: the symmetric scattering-angle distributions around the instantaneous swimming direction, i.e., the distributions $\widetilde{Q}(\varphi)$ for whose single one mode is centered about $\varphi = 0$, or $\pm\pi$; and the asymmetric ones, whose mode is located at some value on the interval $[-\pi, \pi]$, except 0 or π.

1. Symmetric scattering-angle distributions

Smooth-enough unimodal distributions, $\widetilde{Q}_S(\varphi)$, that are symmetrically distributed around the mode $\phi = 0$ or around the mode $\phi = \pm\pi$, are of great interest since there is a variety of biological organisms and artificially designed particles that follow this pattern (strategy) of motion. When the scattered angle is distributed around $\phi = 0$, the motion is highly persistent, and it is perhaps the most ubiquitous pattern of active motion observed. On the contrary, motion becomes highly anti-persistent if the distribution of scattered angles is centered around $\pm\pi$, a pattern of motion known as *run-and-reverse* exhibited by a variety of microorganisms [31]. In both cases we have that $\Omega_n = 0$ for all n, since $\lambda_n^* = \lambda_n$ in this case. For scattered angles that frequently occur forwardly around the instantaneous direction of motion, i.e., when the mode of $\widetilde{Q}_S(\varphi)$ is located at $\phi = 0$, it can be shown that $0 < \Gamma_n \le \Gamma_m$ whenever $n < m$ (see Fig. 2 for some symmetric unimodal distributions). Particularly, we have that $\Gamma_2/\Gamma_1 \ge 1$, and the effects of Γ_2 are revealed in the kurtosis during times before the persistence time (see dotted-dashed lines in Fig. 3 for $\Gamma_2/\Gamma_1 = 10$ and 100, respectively). In such a period of time, the pulse deviates from the initial sharp pulse giving rise to wakes, characteristic of wave-like propagation [15].

On the contrary, for scattered angles that frequently occur around the contrary direction to the instantaneous direction of motion, i.e., when $\phi = \pi$, we get that $\Gamma_2/\Gamma_1 \le 1$ and the effects of Γ_2 are revealed in the kurtosis at times larger than the persistence time (see dashed line in Fig. 3).

These inequalities give a clear insight of the role of the properties of the scattering-angles distribution on the time evolution of the "shape" of $p_0(\boldsymbol{x}, t)$, characterized by its kurtosis $\kappa(t)$. Indeed, the transit from the initial pulse, at the short-time regime, to the Gaussian distribution, in the long-time regime, depends strongly on the ratio Γ_2/Γ_1 as is shown in Fig. 3, where the kurtosis as a function of the dimensionless time, $\Gamma_1 t$, is shown for the following values of Γ_2/Γ_1: 0.1 (dashed-red line), 1 (solid-black line), 10 (dashed-dotted-blue line) and 100 (dashed-doubled-dotted-magenta line).

The case $\Gamma_2/\Gamma_1 = 1$ is of some interest and leads to a
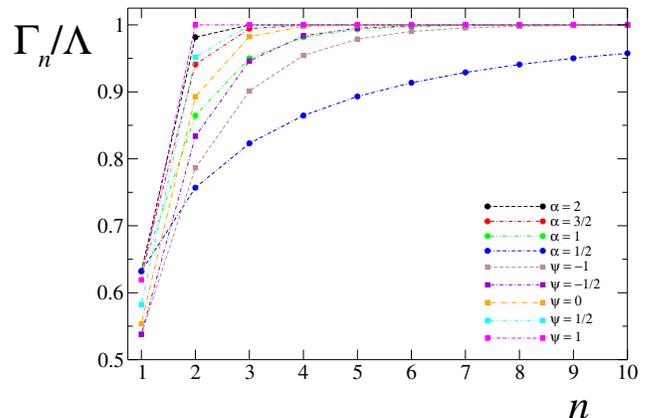
FIG. 2. (Color online) The first ten values of Γ_n/Λ are shown for different unimodal distributions of scattered angles centered at the forward direction of motion. For the Lévy alpha-stable distributions wrapped to the circle, $\widetilde{Q}_{\mathrm{wr}}(\varphi)$, $\alpha = 2$ (wrapped Gaussian), $3/2$, 1 (wrapped Lorentz), and $1/2$ were chosen, all with parameters $\sigma = 1$, $\beta = 0$. For the Jones and Pewsey distributions of scattered angles, $\widetilde{Q}_{\mathrm{JP},\sigma,\phi,\psi}$ the values $\sigma = 1$, $\phi = 0$, and $\psi = -1$ (cardioid), $-1/2$, 0 (von Misses), $1/2$, and 1 (wrapped Cauchy) were chosen.

simple expression for the kurtosis, namely,

$$\kappa(t) = 24 \frac{1 - \Gamma t + \Gamma^2 t^2/3 - e^{-\Gamma t} + \Gamma^2 t^2 e^{-\Gamma t}/6}{[\Gamma t - (1 - e^{-\Gamma t})]^2}, \quad (57)$$

where we have written $\Gamma_1 = \Gamma_2 = \Gamma$. This particular case has, as an instance, the well-known pattern of active motion run-and-tumble, for which $\widetilde{Q}_S(\varphi) = (2\pi)^{-1}$ and $\Gamma_n = \Lambda$ for all n. Notice that the "shape" of $p_0(\boldsymbol{x}, t)$ changes from the initial sharp pulse to the Gaussian distribution in a monotonic way, as can be deduced from the monotonic-non-decreasing time dependence of the kurtosis ($4 \le \kappa(t) \le 8$ at all instant). This monotonic growth is representative of many patterns of active motion for which the direction of motion is slightly scattered from the instantaneous one. For completeness, I have included in Fig. 3 the time dependence of the kurtosis for active Brownian motion [15] (solid-gray line).

For $\Gamma_2 > \Gamma_1$, the transit from the sharp pulse to the Gaussian shape is not monotonic any more (see dashed-dotted-blue line and dashed-doubled-dotted-magenta line in Fig. 3). In the short-time regime, the kurtosis diminishes from the value 4, meaning that wake effects are present in the pulse propagation. Notice the agreement between the kurtosis of the cases considered and the kurtosis for active Brownian motion (solid-gray line) in the long-time regime. For the case when the direction of motion is scattered preferentially in the reverse direction, $\Gamma_2 < \Gamma_1$, the transit from the sharp pulse to the Gaussian distribution is also non-monotonic, but in contrast to the case $\Gamma_2 > \Gamma_1$, the distribution becomes conspicu-
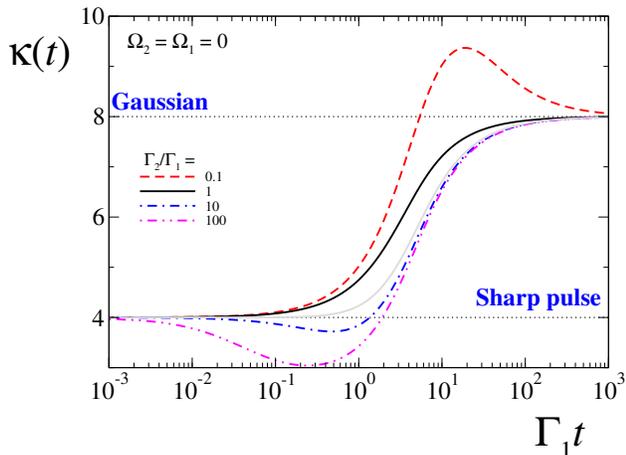
FIG. 3. (Color online) Kurtosis as function of the dimensionless time $\Gamma_1 t$ for $\widetilde{Q}_S$ symmetric scattering-angle distribution, for the values of the ratio $\Gamma_2/\Gamma_1 = 0.1, 1, 10, 100$. Dotted lines mark the values $\kappa = 8$ and 4 that correspond to the cases for which the probability density $p_0(\boldsymbol{x}, t)$ is Gaussian in the long-time regime ($\kappa = 8$), and a sharp pulse that propagates with speed v_0 ($\kappa = 4$), respectively. The solid-gray line corresponds to the time dependence of the kurtosis for active Brownian motion with rotational diffusion constant equal to Γ_1.

ously leptokurtic in the long-time regime tending to the Gaussian asymptotically (dashed-red line).

With this, it is clear from (15) that $\widetilde{P}(\boldsymbol{k}, \varphi, t)$ goes to $(1/2\pi)\widetilde{p}_0(\boldsymbol{k}, t)$ in the long-time limit since in this regime the mode $n = 0$ is the only one that persists.

2. *Asymmetric scattering-angle distributions*

Unimodal distributions that consider a frequent scattering of the swimming direction to directions of motion different from the forward one, or the reverse one, i.e., those that have a mode at angles $\phi \neq 0, \pi$, lead naturally to *circular motion*. Even in the case of forward or reverse scattering, circular motion emerges as consequence of the skewness of the distribution. These statistical considerations allow to describe the motion of *circular swimmers*, which are ubiquitous in nature and have been observed in a variety of biological organisms and of artificially designed swimmers [32–41], and have been of theoretical interest leading to diverse models that describe their motion [25, 42–48].

The particular processes that underly the stationary scattering-angle distribution $\widetilde{Q}(\varphi)$, define the specific values of Γ_1, Γ_2, Ω_1 and Ω_2, whose variations are not independent among them. For instance, for the particular case of the wrapped Gaussian ($\alpha = 2$) with fixed scale parameter $\sigma = 1/4$ and zero skewness, the ratios Γ_2/Γ_1, Ω_1/Γ_1 and Ω_2/Γ_1 are shown in Fig. 4 as functions of ϕ,
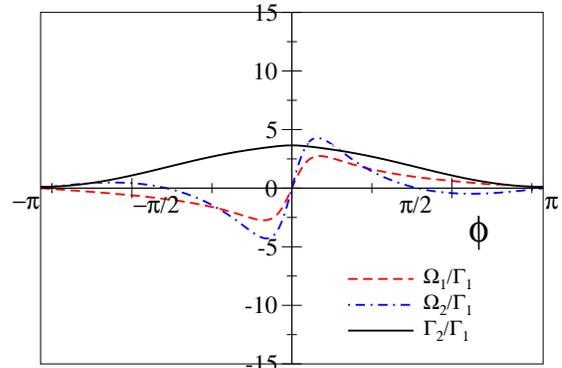
FIG. 4. (Color online) The ratios Γ_2/Γ_1, Ω_1/Γ_1 and Ω_2/Γ_1 are shown as functions of the mode ϕ, when $\widetilde{Q}(\varphi)$ is given by the wrapped-Gaussian distribution (wrapped stable distribution with index $\alpha = 2$), with values of the scale parameter $\sigma = 0.25$ (solid lines) and 0.1 (fuzzy lines).
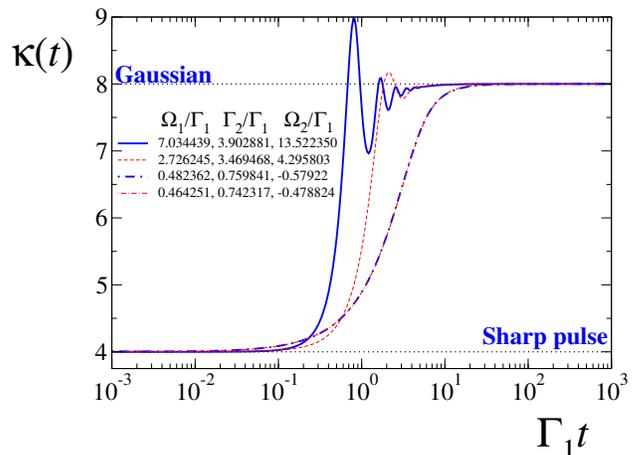
FIG. 5. (Color online) The time dependence of the kurtosis is shown for $\widetilde{Q}(\varphi)$ given by the wrapped-Gaussian distribution (wrapped stable distribution with index $\alpha = 2$), with values of the scale parameter $\sigma = 0.1$ (thick-blue lines) and 0.25 (thin-red lines). The values of the ratios: Γ_2/Γ_1, Ω_1/Γ_1 and Ω_2/Γ_1, correspond to those values of $\phi \in [0, \pi]$, for which Ω_2/Γ_1 is maximum (solid-blue and dashed-red lines) and when is minimum (thick-dotted-dashed and thin-dotted-dashed lines), as can be noticed in Fig. 4.

the value of the mode distribution.

B. Bimodal scattering-angle distributions

It has been observed a variety of organisms that exhibit a bimodal distribution of scattering angles in their

pattern of motion [12, 49], and this bimodality has profound consequences on the spatial distributions of the particles. For the sake of clarifying this, we consider the limit case that corresponds to the bimodal distribution of scattered angles, with modes at the angles φ_1, φ_2, and of zero width, i.e.,

$$\widetilde{Q}(\varphi) = \nu\delta(\varphi - \varphi_1) + (1 - \nu)\delta(\varphi + \varphi_2), \qquad (58)$$

where $0 < \nu < 1$ gives a weighing factor to each mode of the distribution.

1. Symmetrically distributed modes

Consider the bimodal scattering-angle distribution of zero width

$$\widetilde{Q}(\varphi) = \nu\delta(\varphi - \varphi_0) + (1 - \nu)\delta(\varphi + \varphi_0), \qquad (59)$$

where the modes are located symmetrically with respect to the forward direction at $\pm\varphi_0$ with $0 < \varphi_0 < \pi$; and $0 < \nu < 1$ gives the weight of each mode making the scattering-angle distribution asymmetric if $\nu \neq 1/2$. Straightforwardly, we can notice that Γ_n is independent of ν for all n, having $\Lambda(1 - \cos n\varphi_0)$ as its value for given n and φ_0. Notice that the persistence time becomes arbitrarily large as φ_0 vanishes. In contrast, Ω_n does explicitly depend on ν, as $\Lambda(2\nu - 1)\sin n\varphi_0$.

The ratios Γ_2/Γ_1, Ω_1/Γ_1 and Ω_2/Γ_1, that give the full characterization of the kurtosis of the particle position distribution, can be calculated explicitly giving

$$\frac{\Gamma_2}{\Gamma_1} = \left(2\cos\frac{\varphi_0}{2}\right)^2, \qquad (60a)$$

$$\frac{\Omega_1}{\Gamma_1} = (2\nu - 1)\cot\frac{\varphi_0}{2}, \qquad (60b)$$

$$\frac{\Omega_2}{\Gamma_1} = 2(2\nu - 1)\cos\varphi_0\cot\frac{\varphi_0}{2}. \qquad (60c)$$

From these expressions, several diffusive properties in terms of the parameters φ_0 and ν are obtained. Firstly, after setting $\Omega_1/\Gamma_1 = 1$ in Eq. (60b), the maximum value of the effective diffusion coefficient [see Eq. (43)] is obtained whenever $\nu = [1 + \tan(\varphi_0/2)]/2$, with $0 < \varphi_0 < \pi/2$. The contour lines defined by fixing the ratio Ω_1/Γ_1 to a constant χ are shown in Fig. 6.

In Fig. 7, the time dependence of the kurtosis is shown as function of the dimensionless time $\Gamma_1 t$, for the values of the ratios Γ_2/Γ_1 and Ω_2/Γ_1, that correspond to the values of φ_0^* that makes $\nu = 1$ for a given ratio of $\chi = \Omega_1/\Gamma_1$: oscillations are observed for times smaller or of the order of the persistence time for $\chi = 10$, 2 (dashed-dotted lines), for which $\Gamma_2/\Gamma_1 = 3.96$, 3.2 and $\Omega_2/\Gamma_1 = 19.6$, 2.4 respectively. A smooth transition from a sharp pulse and the Gaussian distribution is observed for $\chi = 1$ (maximum effective diffusion coefficient marked by the solid line), for which $\Gamma_2/\Gamma_1 = 2$ and $\Omega_2/\Gamma_1 = 0$. Such a transition is still smooth for $\chi = 0.5$ (thick-dashed line,
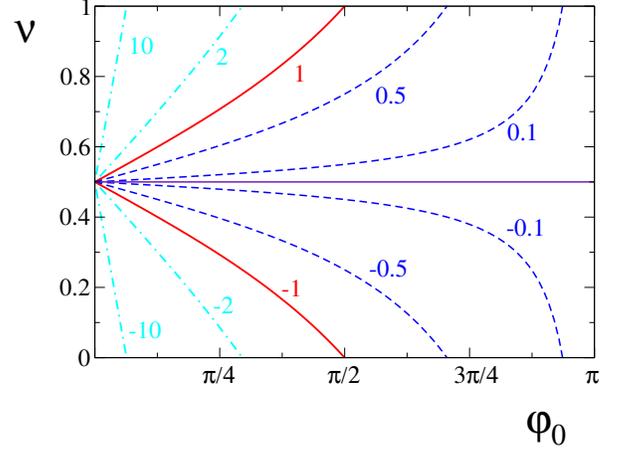
FIG. 6. (Color online) Level curves of constant ratio $\chi = \Omega_1/\Gamma_1$ in the plane ν-φ_0. The solid (red) line corresponds to the case $\Omega_1/\Gamma_1 = 1$ for which the effective diffusion coefficient is maximum. Dashed (blue) lines correspond to the cases for which $|\Omega_1/\Gamma_1| < 1$ (shown $\chi = 10$ and 2), while dashed-dotted (cyan) lines correspond to the cases for which $|\Omega_1/\Gamma_1| > 1$ (shown $\chi = 0.5$ and 0.1).
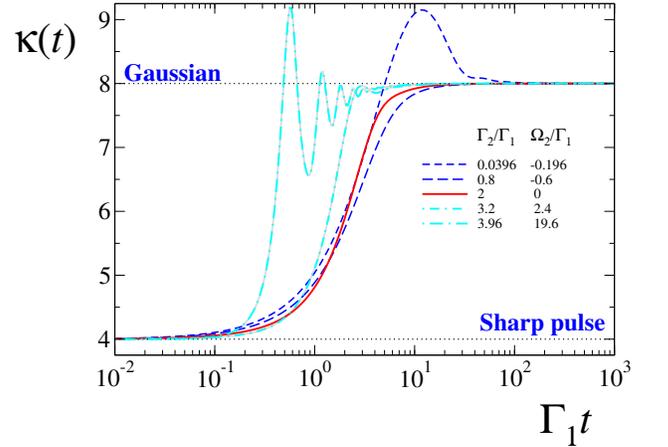
FIG. 7. (Color online) Time dependence of the kurtosis $\kappa(t)$ for the bimodal distribution of scattered angles (59). The values of ratios Γ_2/Γ_1, Ω_2/Γ_1 correspond to the values of φ_0^* that make $\nu = 1$ on the contour lines given in Fig. 6 for the values of $\chi = 10$, 2, 1, 0.5, and 0.1.

$\Gamma_2/\Gamma_1 = 0.8$, $\Omega_2/\Gamma_1 = -0.6$). The transition between the sharp pulse and the Gaussian distribution becomes nonmonotonic again, but now for times larger than the persistence time, when $\chi = 0.1$ (thin-dashed line), for which $\Gamma_2/\Gamma_1 = 0.0396$ and $\Omega_2/\Gamma_1 = -0.196$.
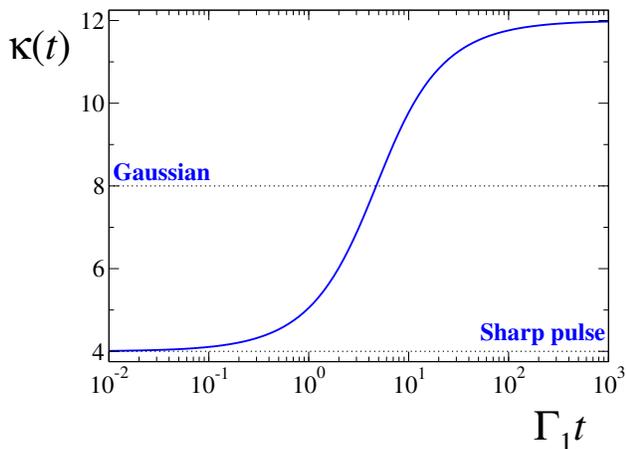
FIG. 8. (Color online) The time dependence of the kurtosis is shown for the bimodal distribution with equally weighed modes at 0 and π, which corresponds to a particular case of the patterns of motion called run-and-reverse.

2. Run-and-reverse

Another instance of a simple bimodal distribution that can be analyzed to some detail, is given by the pattern of motion called *run-and-reverse*. This pattern considers the scattering of the direction of motion along the forward and backward direction, thus having modes at $\phi = 0$ and π, respectively. In the case of zero width distribution, it can be written as

$$\widetilde{Q}(\varphi) = \nu\delta(\varphi) + (1 - \nu)\delta(\varphi - \pi). \quad (61)$$

Notice that Γ_n vanishes for even n, and gives $2\Lambda(1-\nu)$ for odd n, while Ω_n vanishes for all n. The time dependence of the kurtosis can be obtained explicitly in this case,

$$\kappa(t) = 12\frac{6 - 4\Gamma_1 t + \Gamma_1^2 t^2 - 2e^{-\Gamma_1 t}(3 + \Gamma_1 t)}{[\Gamma_1 t - (1 - e^{-\Gamma_1 t})]^2}, \quad (62)$$

and is shown in Fig. 8. Notice that in the asymptotic limit the spatial distribution of the active particles leads to value of the kurtosis 12, which differs conspicuously from the value 8 that characterizes the Gaussian distribution. For this case we have that equation (24) acquires the simple form

$$\widetilde{\mathfrak{D}}(\boldsymbol{k}, \epsilon) = \cfrac{2}{\epsilon + \Gamma + \cfrac{(v_0/2)^2\boldsymbol{k}^2}{\epsilon + \cfrac{(v_0/2)^2\boldsymbol{k}^2}{\epsilon + \Gamma + \cfrac{(v_0/2)^2\boldsymbol{k}^2}{\epsilon + \ddots}}}}. \quad (63)$$

If the width at the modes in Eq. (61) is finite, we recover the Gaussian distribution in the long-time regime, this is clear since although Γ_2 may be small, it is finite.

V. CONCLUSIONS

I have presented a theoretical framework for the statistical analysis of the two-dimensional motion of active swimmers. This framework generalizes existent ones in that considers an arbitrary navigating strategy, that also takes into account circular motion, embedded in the arbitrary distribution of scattered angles of the particle's swimming direction. The framework also complements others, which focus on the time distribution between turning events. The method of solution presented, allowed for an exact analytical expression for the marginal probability distribution of finding a swimmer at $\boldsymbol{x}$ at time t, independently of the direction of motion. Such a solution can be cast as the exact solution of the generalized diffusion equation (23), and an explicit expression for the time-space dependent memory function is presented. This result opens the door to consider the generalized diffusion equation as well-founded to analyze of the motion of active swimmers. Particularly, to consider time-space coupled memory function to describe other variety of patterns of active motion, as the ones described by Lévy walks .

I also presented exact calculations for the time dependence of the mean-square displacement, which depends only on the ratio of the frequency of the circular motion induced by the pattern of active motion, Ω_1, to the persistence time Γ_1. Certainly, there is plenty of the patterns of motion that lead to the same ratio Ω_1/Γ_1, and as such, the mean-square displacement is typical of many of them. However, the differences among different patterns of motion are unveiled in the intermediate-time regime if more information of the pattern of motion is considered (as analyzed for active Brownian motion and run-and-tumble particles in Ref. [8]), and not only those related to $\langle\cos\varphi\rangle_{\widetilde{Q}}$ and $\langle\sin\varphi\rangle_{\widetilde{Q}}$, as is the case for the mean-square displacement.

I showed that consideration of Γ_2 and Ω_2, besides Γ_1 and Ω_1, is enough to distinguish some features among different patterns of motion. Certainly, knowledge of these quantities allows the exact calculation of the time dependence of the kurtosis, which gives information about the "shape" of the particle's position distribution. Some patterns of motion induce a smooth transition with time, from the initial sharp pulse, to the Gaussian of the long-time regime. Others deviate from this behavior and transit, from the initial sharp pulse to the Gaussian distribution, in a rather complex way characterized by oscillations.

Finally, although no exact solution to the Fokker-Planck equation (5) is known, the analysis presented in this paper achieves to give a wide reach understanding of the influence of an arbitrary pattern of motion on the statistical properties of the active swimmers, and encourages the development of more general theoretical frameworks of active motion that allow the incorporation of more general conditions.

ACKNOWLEDGMENTS

[1] J. Taktikos, H. Stark, and V. Zaburdaev, PLoS ONE **8**, 1 (2014), URL http://dx.doi.org/10.1371%2Fjournal.pone.0081936.

[2] F. Detcheverry, EPL (Europhysics Letters) **111**, 60002 (2015), URL http://stacks.iop.org/0295-5075/111/i=6/a=60002.

[3] C. Bechinger, R. Di Leonardo, H. Löwen, C. Reichhardt, G. Volpe, and G. Volpe, Rev. Mod. Phys. **88**, 045006 (2016), URL https://link.aps.org/doi/10.1103/RevModPhys.88.045006.

[4] A. Pototsky and H. Stark, EPL (Europhysics Letters) **98**, 50004 (2012), URL https://doi.org/10.1209%2F0295-5075%2F98%2F50004.

[5] M. E. Cates and J. Tailleur, EPL (Europhysics Letters) **101**, 20010 (2013), URL http://stacks.iop.org/0295-5075/101/i=2/a=20010.

[6] A. P. Solon, M. E. Cates, and J. Tailleur, The European Physical Journal Special Topics **224**, 1231 (2015), ISSN 1951-6401, URL http://dx.doi.org/10.1140/epjst/e2015-02457-0.

[7] H. Stark, The European Physical Journal Special Topics **225**, 2369 (2016), ISSN 1951-6401, URL http://dx.doi.org/10.1140/epjst/e2016-60060-2.

[8] C. Kurzthaler, C. Devailly, J. Arlt, T. Franosch, W. C. K. Poon, V. A. Martinez, and A. T. Brown, Phys. Rev. Lett. **121**, 078001 (2018), URL https://link.aps.org/doi/10.1103/PhysRevLett.121.078001.

[9] F. m. c. Detcheverry, Phys. Rev. E **96**, 012415 (2017), URL https://link.aps.org/doi/10.1103/PhysRevE.96.012415.

[10] J. J. Duderstadt and W. R. Martin, *Transport theory.*, vol. 1 (1979).

[11] J. M. Porra, J. Masoliver, and G. H. Weiss, Physical Review E **55**, 7771 (1997).

[12] M. Theves, J. Taktikos, V. Zaburdaev, H. Stark, and C. Beta, Biophysical Journal **105**, 1915 (2013), ISSN 0006-3495, URL http://www.sciencedirect.com/science/article/pii/S0006349513010217.

[13] G. M. Viswanathan, E. P. Raposo, F. Bartumeus, J. Catalan, and M. G. E. da Luz, Phys. Rev. E **72**, 011111 (2005), URL http://link.aps.org/doi/10.1103/PhysRevE.72.011111.

[14] F. Bartumeus, J. Catalan, G. Viswanathan, E. Raposo, and M. da Luz, Journal of Theoretical Biology **252**, 43 (2008), ISSN 0022-5193, URL http://www.sciencedirect.com/science/article/pii/S0022519308000180.

[15] F. J. Sevilla and L. A. Gómez Nava, Physical Review E **90**, 022130 (2014).

[16] F. J. Sevilla and M. Sandoval, Phys. Rev. E **91**, 052150 (2015), URL http://link.aps.org/doi/10.1103/PhysRevE.91.052150.

[17] F. J. Sevilla, Phys. Rev. E **94**, 062120 (2016), URL http://link.aps.org/doi/10.1103/PhysRevE.94.062120.

[18] S. Mehraeen, B. Sudhanshu, E. F. Koslover, and A. J. Spakowitz, Phys. Rev. E **77**, 061803 (2008), URL https://link.aps.org/doi/10.1103/PhysRevE.77.061803.

[19] F. Detcheverry, The European Physical Journal E **37**, 114 (2014), ISSN 1292-895X, URL https://doi.org/10.1140/epje/i2014-14114-2.

[20] V. Kenkre and F. J. Sevilla, in *Contributions to Mathematical Physics: a Tribute to Gerard G. Emch TS. Ali, KB. Sinha, eds.* (Hindustan Book Agency, New Delhi, 2007), pp. 147–160.

[21] L. Giuggioli, F. Sevilla, and V. Kenkre, Journal of Physics A: Mathematical and Theoretical **42**, 434004 (2009).

[22] S. Goldstein, The Quarterly Journal of Mechanics and Applied Mathematics **4**, 129 (1951), http://qjmam.oxfordjournals.org/content/4/2/129.full.pdf+html, URL http://qjmam.oxfordjournals.org/content/4/2/129.abstract.

[23] V. Zaburdaev, S. Denisov, and J. Klafter, Rev. Mod. Phys. **87**, 483 (2015), URL https://link.aps.org/doi/10.1103/RevModPhys.87.483.

[24] H. Larralde, Phys. Rev. E **56**, 5004 (1997), URL http://link.aps.org/doi/10.1103/PhysRevE.56.5004.

[25] C. Weber, P. K. Radtke, L. Schimansky-Geier, and P. Hänggi, Physical Review E **84**, 011132 (2011).

[26] K. V. Mardia, Sankhyā: The Indian Journal of Statistics, Series B pp. 115–128 (1974).

[27] H. i Wu, B.-L. Li, T. A. Springer, and W. H. Neill, Ecological Modelling **132**, 115 (2000), ISSN 0304-3800, URL http://www.sciencedirect.com/science/article/pii/S0304380000003094.

[28] M. J. Schnitzer, Phys. Rev. E **48**, 2553 (1993), URL http://link.aps.org/doi/10.1103/PhysRevE.48.2553.

[29] B. Hancock and A. Baskaran, Phys. Rev. E **92**, 052143 (2015), URL http://link.aps.org/doi/10.1103/PhysRevE.92.052143.

[30] M. C. Jones and A. Pewsey, Journal of the American Statistical Association **100**, 1422 (2005), http://dx.doi.org/10.1198/016214505000000286, URL http://dx.doi.org/10.1198/016214505000000286.

[31] R. Großmann, F. Peruani, and M. Bär, New Journal of Physics **18**, 043009 (2016), URL https://doi.org/10.1088%2F1367-2630%2F18%2F4%2F043009.

[32] H. C. Crenshaw, Bulletin of Mathematical Biology **55**, 197 (1993), ISSN 0092-8240, URL http://www.sciencedirect.com/science/article/pii/S0092824005800692.

[33] E. Lauga, W. R. DiLuzio, G. M. Whitesides, and H. A. Stone, Biophysical Journal **90**, 400 (2006), ISSN 0006-3495, URL http://www.sciencedirect.com/science/article/pii/S0006349506722214.

[34] V. B. Shenoy, D. T. Tambe, A. Prasad, and J. A. Theriot, Proceedings of the Na-

tional Academy of Sciences **104**, 8229 (2007), http://www.pnas.org/content/104/20/8229.full.pdf, URL `http://www.pnas.org/content/104/20/8229.abstract`.

[35] S. Schmidt, J. van der Gucht, P. M. Biesheuvel, R. Weinkamer, E. Helfer, and A. Fery, European Biophysics Journal **37**, 1361 (2008), ISSN 1432-1017, URL `http://dx.doi.org/10.1007/s00249-008-0340-x`.

[36] B. M. Friedrich and F. Jülicher, New Journal of Physics **10**, 123025 (2008), URL `http://stacks.iop.org/1367-2630/10/i=12/a=123025`.

[37] N. A. Marine, P. M. Wheat, J. Ault, and J. D. Posner, Phys. Rev. E **87**, 052305 (2013), URL `http://link.aps.org/doi/10.1103/PhysRevE.87.052305`.

[38] F. Kümmel, B. ten Hagen, R. Wittkowski, I. Buttinoni, R. Eichhorn, G. Volpe, H. Löwen, and C. Bechinger, Phys. Rev. Lett. **110**, 198302 (2013), URL `http://link.aps.org/doi/10.1103/PhysRevLett.110.198302`.

[39] D. Takagi, A. B. Braunschweig, J. Zhang, and M. J. Shelley, Phys. Rev. Lett. **110**, 038301 (2013), URL `https://link.aps.org/doi/10.1103/PhysRevLett.110.038301`.

[40] J. R. Gomez-Solano, A. Blokhuis, and C. Bechinger, Phys. Rev. Lett. **116**, 138301 (2016), URL `https://link.aps.org/doi/10.1103/PhysRevLett.116.138301`.

[41] N. Narinder, C. Bechinger, and J. R. Gomez-Solano, Phys. Rev. Lett. **121**, 078003 (2018), URL `https://link.aps.org/doi/10.1103/PhysRevLett.121.078003`.

[42] S. van Teeffelen and H. Löwen, Phys. Rev. E **78**, 020101(R) (2008), URL `http://link.aps.org/doi/10.1103/PhysRevE.78.020101`.

[43] B. M. Friedrich and F. Jülicher, Phys. Rev. Lett. **103**, 068102 (2009), URL `http://link.aps.org/doi/10.1103/PhysRevLett.103.068102`.

[44] T. Ohta and T. Ohkuma, Phys. Rev. Lett. **102**, 154101 (2009), URL `https://link.aps.org/doi/10.1103/PhysRevLett.102.154101`.

[45] R. Wittkowski and H. Löwen, Phys. Rev. E **85**, 021406 (2012), URL `http://link.aps.org/doi/10.1103/PhysRevE.85.021406`.

[46] R. Ledesma-Aguilar, H. Löwen, and J. M. Yeomans, The European Physical Journal E **35**, 1 (2012), ISSN 1292-895X, URL `http://dx.doi.org/10.1140/epje/i2012-12070-5`.

[47] H. Löwen, The European Physical Journal Special Topics **225**, 2319 (2016), ISSN 1951-6401, URL `https://doi.org/10.1140/epjst/e2016-60054-6`.

[48] C. Kurzthaler and T. Franosch, Soft Matter pp. – (2017), URL `http://dx.doi.org/10.1039/C7SM00873B`.

[49] K. J. Duffy and R. M. Ford, Journal of bacteriology **179**, 1428 (1997).